Accepted version of of: W. P. du Plessis, “Platform Skin Return and Retrodirective Cross-Eye Jamming,” *IEEE Transactions on Aerospace and Electronic Systems*, vol. 48, no. 1, pp. 490-501, January 2012. Published version is available online at: http://ieeexplore.ieee.org/arnumber=6129650

Platform Skin Return and Retrodirective Cross-Eye Jamming

W. P. du Plessis, *Senior Member, IEEE*

Abstract

The effect of platform skin return on retrodirective cross-eye jamming is analysed, allowing the parameters of a cross-eye jammer in the presence of skin return to be determined. The inherently unknown phase of the platform skin return is accounted for, and the effect of variations in Jammer-to-Signal Ratio (JSR) is investigated. The widely-held, though unsubstantiated, view that a JSR of 20 dB is required for effective cross-eye jamming is found to be reasonable, though conservative.

Index Terms

Electronic warfare, electronic countermeasures, radar countermeasures, radar tracking, monopulse radar.

I. Introduction

Cross-eye jamming is an angular deception technique that attempts to deceive a tracking radar as to the true position of its target by recreating the worst-case angular error due to glint [1]–[14]. In fact, cross-eye jamming is occasionally referred to as "artificial glint" [1]–[3].

Glint is a phenomenon that affects all radars and is caused by interference between the returns from a number of points on a radar target [15], [16]. A number of glint analyses have been developed [17]–[21], and they have been shown to be equivalent [22]–[24].

A cross-eye jammer is implemented by transmitting signals which have roughly equal amplitude and which are ideally 180° of out phase from two antennas to emulate the case of glint that gives the largest angular error [2]–[14]. The jammer antenna separation must be as large as possible because the induced error is a function of the jammer antenna spacing [6]–[8].

Given that cross-eye jamming originated as an attempt to recreate glint, it is not surprising that one of the earliest glint analyses, the phase-front analysis of glint [17], is usually used to analyse and explain cross-eye jamming [2], [5], [6], [11], [12]. However, it has recently been shown that the accuracy of glint analyses when applied to cross-eye jamming is limited by a number of assumptions [7]–[9]. (Note that this statement does not imply that glint analyses are inaccurate when applied to glint as this is clearly not true [16].)

Manuscript received May 10, 2010; revised September 28, 2010. This work was supported by the Armaments Corporation of South Africa (Armscor) under contract KT521896.

W. P. du Plessis is with Defence, Peace, Safety and Security (DPSS), at the Council for Scientific and Industrial Research (CSIR), Pretoria, 0001, South Africa (e-mail: wduplessis@csir.co.za).

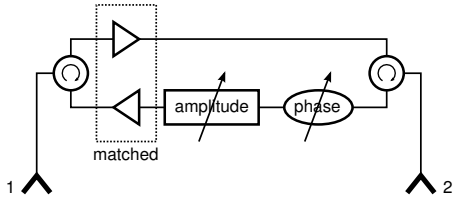

Fig. 1. The retrodirective implementation of a cross-eye jammer. In the ideal isolated case, the amplitudes should be matched and the phase shifts should differ by 180°.

The main limitation of glint analyses when applied to cross-eye jamming is that the retrodirective implementation of cross-eye jamming (shown in Fig. 1) is not accounted for [8]. This limitation is crucial because the retrodirective implementation appears to be the only practical way of realising a cross-eye jammer, and in fact, most of the cross-eye literature only considers the retrodirective case [4]–[11] despite the fact that other options exist [1], [2]. The main reason for this is that other cross-eye jammer implementations place extreme, impractical tolerances on cross-eye jammer systems [4], [5].

The case where the return from a cross-eye jammer must compete with the skin return from the platform mounting the jammer has not been widely considered in the literature apart from vague statements that high Jammer-to-Signal Ratios (JSRs) are required for cross-eye jamming to be effective [2]–[6]. While a value of at least 20 dB is widely quoted [3]–[6], the basis for this value is unclear. Three analyses of cross-eye jamming in the presence of platform skin return exist, but they are of limited value.

The first approach is to consider the cross-eye jammer as a point source in the direction of the error predicted by the glint analysis, and then to use the relative amplitudes of the cross-eye jammer signal and the platform skin return to determine their combined effect [1], [11]. The main drawback of this approach is that, as highlighted above, the conventional glint analyses have limited accuracy when applied to cross-eye jamming, so the accuracy of this approach is limited. A further limitation is that this approach ignores the fact that the signals add in the sum- and difference-channel returns rather than as monopulse ratios.

The second approach is to approximate the difference-channel antenna pattern by a quadratic function in the direction of the target and jammer [10]. While this approach is reasonable, the analysis in [10] predicts that an amplitude match of 0.05 dB with a perfect phase match or a phase match of 0.3° with a perfect amplitude match are required for a cross-eye jammer to achieve half the error of a perfectly-matched isolated cross-eye jammer. Such accurate matching is impossible to achieve outside a laboratory, yet cross-eye jammers have been demonstrated in the field [12], [25], so the accuracy of this analysis is questionable.

The third approach for considering the platform skin return is to extend one of the glint analyses to consider the platform skin return as a third scatterer. This has been done for the glint analysis that uses linear fits to the monopulse antenna patterns [20], [21] and the results are presented in [26]. This work found that almost no error is encountered for a JSR of 10 dB, while large errors are encountered for a JSR of 30 dB. However, this approach suffers from the same inaccuracies as all other glint analyses when applied to cross-eye jamming, so the accuracy of these results is questionable. A further limitation of the results presented in [26] is that the equations derived have extremely complex mathematical forms and the graphs provided have limited value to the designer of a cross-eye jammer.

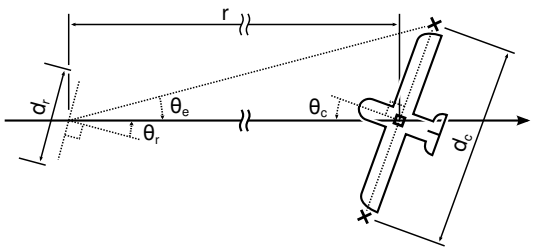

Fig. 2. The geometry of the cross-eye jamming scenario considered. The radar and jammer antenna element phase centres are denoted by circles and crosses respectively, and the point target used to model the platform is denoted by a square.

This paper presents results that overcome the limitations of the existing literature by quantifying the effect of platform skin return on a retrodirective cross-eye jammer. The results are based on the analysis presented in [7]–[9] and thus do not suffer from the inaccuracies that affect other glint analyses. Both the effects of the cross-eye jammer and platform skin return parameters are considered in detail. The results are presented graphically to allow visualisation of the effect of platform skin return on the performance of a retrodirective cross-eye jammer.

The process used to analyse cross-eye jamming in the presence of platform skin return is outlined in Section II. Section III presents results computed using the approach described in Section II and provides a number of useful graphs. Finally brief conclusions are given in Section IV.

II. Mathematical Analysis

Equations describing the effect of platform skin return on the operation of a retrodirective cross-eye jammer are derived in this section based on the analysis described in [7], [8]. The system configuration is shown in Fig. 2 with the radar on the left and the jammer system and the platform it is mounted on (an aircraft in this case) on the right.

While only phase-comparison monopulse is considered below, results for the phase-comparison case have been shown to be applicable to any monopulse radar [8], [27].

A. Skin Return

The normalised sum- and difference-channel antenna gains in a direction θ_r measured from boresight are given by [21]

$$S_g = P_r(\theta_r)\cos\left[\beta\frac{d_r}{2}\sin(\theta_r)\right] \tag{1}$$

$$D_g = jP_r(\theta_r)\sin\left[\beta\frac{d_r}{2}\sin(\theta_r)\right] \tag{2}$$

for a phase-comparison monopulse radar where $P_r(\theta_r)$ is the normalised gain of the two antenna elements comprising the radar and the remaining parameters are defined in Fig. 2. The monopulse ratio for a point target at $\theta_r = 0$ is given by [21]

$$M_r = \Im\left\{\frac{D_g}{S_g}\right\} \tag{3}$$

$$= \tan\left[\beta\frac{d_r}{2}\sin(\theta_r)\right] \tag{4}$$

when an exact monopulse processor is considered. The monopulse indicated angle is determined by solving (3) and (4) for θ_r given the necessary parameters [21].

The fact that the radar transmits using the sum-channel antenna beam does not need to be explicity considered here because the illumination is common to both the sum- and difference-channel returns and thus cancels when the monopulse ratio is computed.

B. Jammer Return

The normalised sum- and difference-channel returns for the cross-eye jammer in isolation with the jammer antennas positioned symmetrically around $\theta_r = 0$ as shown in Fig. 2 are given by [7], [8]

$$S_j = P_r\left(\theta_r - \theta_e\right) P_c\left(\theta_c - \theta_e\right) P_r\left(\theta_r + \theta_e\right) P_c\left(\theta_c + \theta_e\right) \times \frac{1}{2}\left(1 + ae^{j\phi}\right)\left[\cos\left(2k\right) + \cos\left(2k_c\right)\right] \tag{5}$$

$$D_j = P_r\left(\theta_r - \theta_e\right) P_c\left(\theta_c - \theta_e\right) P_r\left(\theta_r + \theta_e\right) P_c\left(\theta_c + \theta_e\right) \times j\frac{1}{2}\left[\left(1 + ae^{j\phi}\right)\sin\left(2k\right) + \left(1 - ae^{j\phi}\right)\sin\left(2k_c\right)\right] \tag{6}$$

where $P_c\left(\theta\right)$ is the normalised gain of the cross-eye jammer antenna elements with the angle measured from broadside,

$$k = \beta\frac{d_r}{2}\sin\left(\theta_r\right)\cos\left(\theta_e\right) \tag{7}$$

$$\approx \beta\frac{d_r}{2}\sin\left(\theta_r\right) \tag{8}$$

$$k_c = \beta\frac{d_r}{2}\cos\left(\theta_r\right)\sin\left(\theta_e\right) \tag{9}$$

$$\approx \beta\frac{d_r}{2}\cos\left(\theta_r\right)\theta_e \tag{10}$$

$$\theta_e \approx \frac{d_c}{2r}\cos\left(\theta_c\right) \tag{11}$$

where the approximations are extremely accurate because $d_c \ll r$ making θ_e very small. The monopulse ratio is given by [7]

$$M_j = \frac{\sin\left(2k\right) + \sin\left(2k_c\right)G_C}{\cos\left(2k\right) + \cos\left(2k_c\right)} \tag{12}$$

with the cross-eye gain G_C being given by [6]

$$G_C = \frac{1 - a^2}{1 + a^2 + 2a\cos\left(\phi\right)} \tag{13}$$

where a and ϕ are the relative amplitude and phase of the two directions through the retrodirective cross-eye jammer shown in Fig. 1. This means that the signal received at antenna 2 and transmitted from antenna 1 in Fig. 1 will have an amplitude scaling of a and a phase shift of ϕ relative to the signal received at antenna 1 and transmitted from antenna 2 in Fig. 1

C. Total Return

At this stage, it is tempting to simply add the monopulse processor outputs given in (4) and (12) to determine the output of the monopulse error for both the platform and the cross-eye jammer. In fact, this is effectively what is done in [1], [11]. However, this approach is incorrect because the signals add in the sum and difference channels, and a monopulse processor uses these sums to form its output.

The jammer sum- and difference-channel returns in (5) and (6) include the effect of the sum channel on transmission to properly model the retrodirective nature of the cross-eye jammer. The sum- and difference-channel returns for the platform skin return must thus be multiplied by the sum-channel antenna gain to ensure that they are equivalent to the jammer results. The total sum- and difference-channel returns for both the platform and the cross-eye jammer are thus

$$\begin{aligned} S_t &= S_j + a_s e^{j\phi_s} S_g^2 && (14)\\ &= \frac{1}{2}\left[P_r\left(\theta_r\right)\right]^2 \left(1 + ae^{j\phi}\right)\left[\cos\left(2k\right) + 1\right] + \\ &\qquad a_s e^{j\phi_s} \frac{1}{2}\left[P_r\left(\theta_r\right)\right]^2 \left\{\cos\left[\beta d_r \sin\left(\theta_r\right)\right] + 1\right\} && (15)\\ &\approx \frac{1}{2}\left[P_r\left(\theta_r\right)\right]^2 \left\{\left(1 + ae^{j\phi} + a_s e^{j\phi_s}\right)\left[\cos\left(2k\right) + 1\right]\right\} && (16) \end{aligned}$$

$$\begin{aligned} D_t &= D_j + a_s e^{j\phi_s} S_g D_g && (17)\\ &= j\frac{1}{2}\left[P_r\left(\theta_r\right)\right]^2 \left[\left(1 + ae^{j\phi}\right)\sin\left(2k\right) + \right. \\ &\qquad \left. \left(1 - ae^{j\phi}\right)\sin\left(2k_c\right)\right] + \\ &\qquad j\frac{1}{2}\left[P_r\left(\theta_r\right)\right]^2 a_s e^{j\phi_s} \sin\left[\beta d_r \sin\left(\theta_r\right)\right] && (18)\\ &\approx j\frac{1}{2}\left[P_r\left(\theta_r\right)\right]^2 \left[\left(1 + ae^{j\phi} + a_s e^{j\phi_s}\right)\sin\left(2k\right) + \right. \\ &\qquad \left. \left(1 - ae^{j\phi}\right)\sin\left(2k_c\right)\right] && (19) \end{aligned}$$

where the platform skin return will have an amplitude scaling of a_s and phase shift of ϕ_s relative to the return from one direction through the cross-eye jammer (i.e. $a = 0$). Given that (16) and (19) were derived from (1) and (2), these results implicitly model the platform skin return using a point target halfway between the jammer antennas.

The following approximations are made to obtain (16) and (19) under the assumption that θ_e is small:

1) the approximate form of k in (8),
2) $P_r\left(\theta_r - \theta_e\right) P_r\left(\theta_r + \theta_e\right) \approx \left[P_r\left(\theta_r\right)\right]^2$,
3) $P_c\left(\theta_c - \theta_e\right) P_c\left(\theta_c + \theta_e\right) \approx \left[P_c\left(\theta_c\right)\right]^2 \approx 1$ because the jammer antenna gain is included in the calculation of the JSR in Section II-E, and
4) $\cos\left(2k_c\right) \approx 1$.

Approximation 4 is the least accurate of these approximations and will dominate the accuracy of results based on (16) and (19).

The error caused by assumption 4 above is the difference between the exact and approximate total sum-

channel returns in (14) and (16) respectively, and is given by

$$\Delta S_t = \frac{1}{2}\left[P_r\left(\theta_r\right)\right]^2 \left\{\left(1+ae^{j\phi}\right)\left[\cos\left(2k_c\right)-1\right]\right\} \tag{20}$$

where ΔS_t is the error when the other assumptions listed above are accurate. The effect of the error in (20) will be negligible as long as ΔS_t is a small proportion of S_t, which can be written as

$$\left|\frac{\Delta S_t}{S_t}\right| \ll 1 \tag{21}$$

$$\left|\frac{\left(1+ae^{j\phi}\right)\left[\cos\left(2k_c\right)-1\right]}{\left(1+ae^{j\phi}+a_s e^{j\phi_s}\right)\left[\cos\left(2k\right)+1\right]}\right| \ll 1\,. \tag{22}$$

The relationship in (22) will hold when:

1) the jammer antenna separation is much smaller than the radar's sum-channel beamwidth ($\theta_e \ll \beta d_r$, so $2k_c$ is very small and $\cos\left(2k_c\right) \approx 1$, making the numerator of (22) small),
2) the jammer is near the radar's boresight direction ($\beta d_r \sin\left(\theta_r\right)$ is far from π, so $\cos\left(2k\right)$ is not close to -1 ensuring that the denominator of (22) is not small), and
3) the sum-channel jammer return and the sum-channel skin return do not cancel ($1+ae^{j\phi}+a_s e^{j\phi_s}$ is not small enough to violate the relationship in (22)).

Conditions 1 and 2 are both reasonable and do not seriously limit the validity of the sum-channel approximation in (16). However, condition 3 can occur in practical cross-eye jammers.

Condition 3 will be violated when the sum-channel return becomes negligibly small, causing the monopulse ratio and indicated angle to be subject to extremely large variations. This situation is obviously not desirable for a practical cross-eye jammer, but it can occur at surprisingly low JSRs. For example, a retrodirective cross-eye jammer with a relative amplitude (a) and phase (ϕ) of 1 dB and 180° respectively will have a total sum-channel return which is 19.3 dB below the jammer signals in isolation. Under the correct phase conditions, a JSR of 20 dB (see Section II-E below) can lead to a total sum-channel return that is more than 40 dB below the jammer signals in isolation and 20 dB below the platform skin return.

However, while violating condition 3 will lead to large variations in the extreme values of the monopulse ratio and indicated angle, it will not have a noticeable effect on the median value of either of these parameters. The main results below are based on the median monopulse ratio and indicated angle values, so the accuracy of these results only depends on conditions 1 and 2 which are much less restrictive than condition 3.

From (3), (16) and (19), the total monopulse ratio can be approximated by

$$M_t \approx \tan\left(k\right) + \Re\left\{\frac{1-ae^{j\phi}}{1+ae^{j\phi}+a_s e^{j\phi_s}}\right\}\frac{\sin\left(2k_c\right)}{\cos\left(2k\right)+1} \tag{23}$$

where the relationship [28]

$$\tan\left(k\right) = \frac{\sin\left(2k\right)}{\cos\left(2k\right)+1} \tag{24}$$

was used. The accuracy of (23) will be comparable to the accuracy of (16) because (19) does not include approximation 4. The form of (23) is similar to (12) because the first term acts as a beacon while the second term causes an angular error [7], [8].

The error portion of the monopulse ratio in (23) consists of two factors, one of which depends on the jammer parameters and the Radar Cross Section (RCS) of the platform (a, ϕ, a_s and ϕ_s) while the other depends on

the geometry of the engagement (the parameters in Fig. 2 via k and k_c). The geometry of an engagement is fixed by physical constraints, though the jammer antenna element spacing should be made as large as possible to induce a large angular error in the radar being jammed [1]–[8], [10]–[14].

The analysis of the effect of the jammer parameters and platform RCS on the induced angular error is complicated by the fact that the phase of the platform RCS is impossible to specify or determine with certainty. This is because RCS depends on reflections from a number of scatterers on a platform, and even physically small relative movements of these scatterers due to vibration and manoeuvre can cause large variations in the RCS – the basis of glint [15], [16]. While these RCS variations also affect the magnitude of the RCS, it is possible to determine a maximum RCS magnitude which is never exceeded, and the RCS of military systems is specified in this way.

D. Total Cross-Eye Gain

By noting that (12) reduces to the same form as (23) when $\cos(2k_c) \approx 1$, it can be seen that the term

$$G_{Ct} = \Re\left\{\frac{1 - ae^{j\phi}}{1 + ae^{j\phi} + a_s e^{j\phi_s}}\right\} \tag{25}$$

fulfils the same role in (23) as the cross-eye gain in (12). Equation (25) is thus used to define the total cross-eye gain G_{Ct}.

The numerator in (25) is related to the portion of the difference-channel return in (6) and (19) that causes an error, and the denominator is determined by the total sum-channel return in (16). The fact that the real part of (25) is used means that only the portion of the numerator that is in phase with the denominator is considered. The jammer must thus dominate the sum-channel return to control the relative phases of the numerator and denominator of (25).

Defining a_j and ϕ_j by

$$a_j e^{j\phi_j} = \frac{a_s e^{j\phi_s}}{1 + ae^{j\phi}} \tag{26}$$

gives the skin return parameters relative to the sum-channel return of the cross-eye jammer. The magnitude of (26) can be written as

$$a_j = \frac{a_s}{|1 + ae^{j\phi}|} \tag{27}$$

$$= \frac{a_s}{\sqrt{1 + a^2 + 2a\cos(\phi)}}. \tag{28}$$

Substituting (26) into (25) allows the total cross-eye gain to be rewritten as

$$G_{Ct} = \Re\left\{\frac{1 - ae^{j\phi}}{(1 + ae^{j\phi})(1 + a_j e^{j\phi_j})}\right\} \tag{29}$$

$$= \frac{\left(1 - a^2\right)\left[1 + a_j\cos(\phi_j)\right] - 2aa_j\sin(\phi)\sin(\phi_j)}{\left[1 + a^2 + 2a\cos(\phi)\right]\left[1 + a_j^2 + 2a_j\cos(\phi_j)\right]}. \tag{30}$$

While it is tempting to assume that the last term in the numerator of (30) is negligible, this assumption is not accurate unless ϕ is very close to π.

Using the result derived in the appendix, the median of (30) can be shown to be

$$G_{Ctm} = \frac{1 - a^2}{\left[1 + a^2 + 2a\cos(\phi)\right]\left(1 + a_j^2\right)} \tag{31}$$

$$= G_C \cdot K_S \tag{32}$$

where the subscript m has been added to indicate median value and K_S is an effectiveness factor given by

$$K_S = \frac{1}{1 + a_j^2}\,. \tag{33}$$

The effectiveness factor determines what proportion of the isolated cross-eye gain is achieved in the median case when skin return is present. The median total cross-eye gain can also be written as

$$G_{Ctm} = \frac{1 - a^2}{1 + a^2 + 2a\cos(\phi) + a_s^2} \tag{34}$$

where (28) was used to simplify the result.

While the above results are exact, the definition of the total cross-eye gain is based on (23) which is approximate. However, as shown above, (23) is accurate in the median case.

E. Jammer-to-Signal Ratio

The JSR of a cross-eye jammer is the ratio of one of the jammer transmitters operating in isolation to the platform skin return [6], [10]. The JSR can thus be determined from (16) by setting $a = 0$ giving

$$\text{JSR} = \frac{1}{a_s^2}\,. \tag{35}$$

Note that $a = 0$ is only required for the calculation of the JSR and does not imply that the jammer will be realised with this parameter value. The definition of the JSR above implies that $a \leq 1$ to ensure that the stronger of the two directions through the jammer is used to compute the JSR.

In terms of the parameters of the jammer components, the JSR of one of the directions through a cross-eye jammer given by [11]

$$\text{JSR} = \frac{[\lambda G_J]^2\, G_A}{4\pi\sigma_p} \tag{36}$$

when the jammer is operating in linear mode (output power is a linear function of input power) where λ is the wavelength, G_J is the gain of the jammer antennas in the direction of the radar, G_A is the gain of the system connecting the two jammer antennas and σ_p is the platform RCS, and by [11]

$$\text{JSR} = \frac{P_J G_J}{P_R G_R} \cdot \frac{4\pi r^2}{\sigma_p} \tag{37}$$

when the jammer is operating in saturated mode (maximum output power) where P_J and P_R are the jammer and radar power respectively, G_R is the radar antenna gain in the direction of the jammer and r is the range from the radar to the jammer. The value of a_s can now be determined from (35) and either (36) or (37).

The JSR can be written as a function of the effectiveness factor by solving (33) for a_j and using (28) and (35) to give

$$\text{JSR} = \frac{1}{[1 + a^2 + 2a\cos(\phi)]} \cdot \frac{K_S}{(1 - K_S)} \tag{38}$$

which allows the JSR to achieve a specified effectiveness factor to be determined directly. When $K_S = 0.5$, (38) becomes

$$\text{JSR} = \frac{1}{[1 + a^2 + 2a\cos(\phi)]}, \qquad \text{when } K_S = 0.5 \tag{39}$$

which is useful to determine the JSR required to make the median total cross-eye gain half the isolated cross-eye gain.

The JSR can also be written as a function of the median total cross-eye gain by solving (34) for a_s and substituting the result into (35) giving

$$a_s^2 = \frac{1-a^2}{G_{Ctm}} - \left[1 + a^2 + 2a\cos\left(\phi\right)\right] \tag{40}$$

$$\text{JSR} = \frac{G_{Ctm}}{1 - a^2 - \left[1 + a^2 + 2a\cos\left(\phi\right)\right] G_{Ctm}} \tag{41}$$

thereby allowing the JSR to achieve a given median performance to be calculated directly.

III. Results

Results that validate the accuracy of the approximations made in Section II-C are presented in Section III-A. The effect of the presence of platform skin return on the indicated angle is given in Section III-B, and a consideration of how the total cross-eye gain is affected by skin return is presented in Section III-C.

This section will consider the following scenario whose parameters are typical of a missile engaging an aircraft or ship [7]:

- X-Band radar (frequency is 10 GHz),
- 10° radar beamwidth ($d_r = 2.54$ wavelengths, and each radar antenna element is a uniformly excited aperture 2.54 wavelengths long),
- 1 km jammer range ($r = 1$ km),
- 10 m jammer element separation ($d_c = 10$ m), and
- 30° jammer rotation ($\theta_c = 30^\circ$).

The relative amplitude (a) and phase (ϕ) of the two directions through the retrodirective cross-eye jammer and the JSR of the jammer will be indicated on the figures.

As stated in Section II-C, it is impossible to know a platform's RCS phase with any accuracy because vibrations and other minor variations can have a very large effect on the phase of the RCS. The numerical results reported in this section were generated using 10^6 values of ϕ_s equally spaced over the range $0^\circ \leq \phi_s < 360^\circ$.

A. Accuracy of Approximations

The accuracy of the approximations made during the derivation of (23) was shown to be good in the median case in Section II-C, and this section presents results validating this conclusion.

The cross-eye jamming scenario described above is modified in this section as follows:

- K-Band radar (frequency is 20 GHz),
- 5° radar beamwidth ($d_r = 5.08$ wavelengths, and each radar antenna element is a uniformly excited aperture 5.08 wavelengths long),
- 20 m jammer element separation ($d_c = 20$ m), and
- 0° jammer rotation ($\theta_c = 0^\circ$).

These changes were introduced to test an extreme case of the validity of the approximations made during the derivation of (23). The jammer antenna element spacing ($2\theta_e$) is 1.15° which corresponds to 22.9% of the sum-channel 3-dB antenna beamwidth – a very large value that is unlikely to occur in practice.

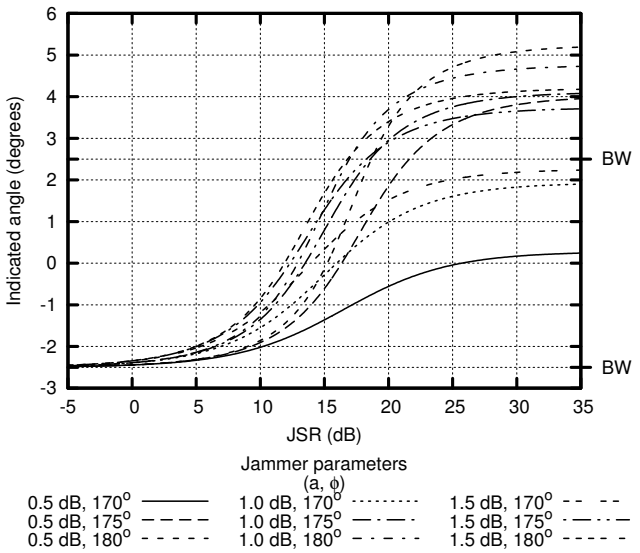

(a) Numerical results. The extent of the radar's sum-channel 3-dB beamwidth is marked "BW" on the right axis.

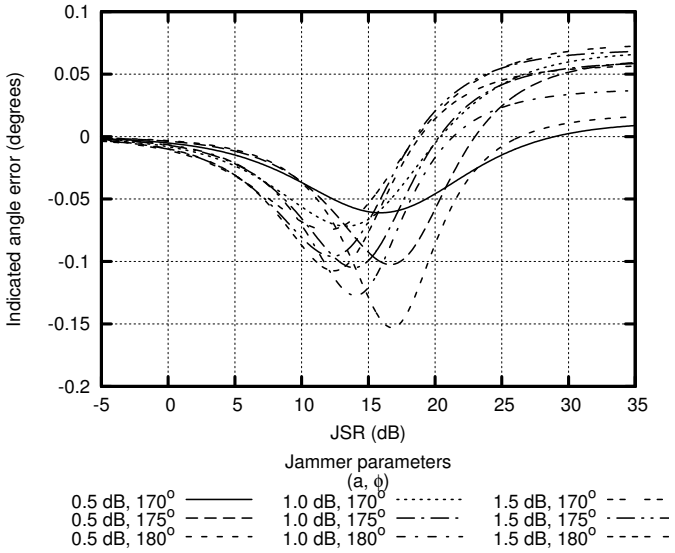

(b) Difference between the numerical and analytic results.

Fig. 3. Comparison between indicated-angle results obtained numerically using (14) and (17), and the analytic results using (23) and (34).

The above parameters highlight the approximations inherent in the second term of (23). The approximations inherent in the first term of (23) are emphasised by positioning jammer and platform on one edge of the radar's sum-channel 3-dB beamwidth at -2.5°.

The median indicated angle obtained numerically using (3), (4), (14) and (17) is plotted in Fig. 3(a), and the difference between the numerical and approximate median indicated angles obtained using (4) and (23) are shown in Fig. 3(b).

The indicated angle plots in Fig. 3(a) show that a very wide range of indicated angles are obtained, with the largest errors being significantly greater than the radar's sum-channel 3-dB beamwidth. The error is small in all cases despite this extremely large range of indicated angles and the fact that this is an extreme case which is

unlikely to occur in practice. The largest error magnitude is less than 0.16° which is only 3.2% of the radar's sum-channel 3-dB beamwidth.

The approximation in (23) is thus extremely accurate in the median case, even with the extreme parameter values considered here.

B. Indicated Angle Variation

Fig. 4 gives an indication of the variation in the induced indicated angle by plotting the minimum, median and maximum values along with the values that bound three quarters of the result for a target that is on boresight. The three-quarter curves are labelled "25%" and "75%" because 25% and 75% of the results are less than these curves respectively. The minimum, median and maximum curves could be labelled "0%," "50%" and "100%" respectively under this scheme.

The variation is seen to be extremely small when the platform skin return or cross-eye jammer return dominate the results at low and high JSR respectively. However, when the total jammer and platform sum-channel returns have similar magnitudes, the total sum-channel return can become small leading to large monopulse ratios and indicated angles, as discussed in Section II-C.

The JSR values where the amplitudes of the total jammer and platform sum-channel returns have equal amplitudes are marked with additional, unlabelled vertical gridlines in Fig. 4, and the largest variations between the minimum and maximum indicated angles are seen to occur at these JSR values. Furthermore, the extremes of the null-to-null sum-channel antenna beamwidth are denoted "N" on the right axis in Fig. 4, and the range of indicated angles produced in these extreme cases is seen to cover this entire range. While the extreme values display large variations, the central 50% of the distribution bounded by the curves labelled "25%" and "75%" displays a much smaller variation, so large variations are limited to the tails of the distributions.

The discontinuity in the minimum and maximum value plots in Fig. 4(c) can be explained by noting that the total cross-eye gain is given by

$$G_{Ct} = \Re\left\{\frac{1+a}{(1-a)+a_s e^{j\phi_s}}\right\}, \qquad \text{when } \phi = \pi \tag{42}$$

when $\phi = 180^\circ$. From (42), it can be seen that the extreme values of G_{Ct} occur when $\phi_s = 180^\circ$ because this leads to the smallest denominator, giving

$$G_{Ct} = \Re\left\{\frac{1+a}{(1-a)-a_s}\right\}, \qquad \text{when } \phi = \phi_s = \pi \tag{43}$$

which has a denominator very close to zero because the magnitude of the total jammer return $(1-a)$ is very similar to the magnitude of the skin return a_s. When a_s is marginally larger than $(1-a)$, the sign of (43) is negative leading to extreme negative indicated angles and vice versa as seen in Fig. 4(c). The extreme values in Figs 4(a) and 4(b) display similar characteristics, though without the clear discontinuity seen in Fig. 4(c).

C. Median Total Cross-Eye Gain

The median total cross-eye gain is plotted for a number of combinations of jammer parameters in Fig. 5. The total cross-eye gain varies from 0 at low JSRs to much larger values at high JSRs, as expected.

The most important point that arises from Fig. 5 is that the total cross-eye gain is greater than 1 in the majority of the cases considered for surprisingly low JSR values of less than 10 dB. A cross-eye gain of greater

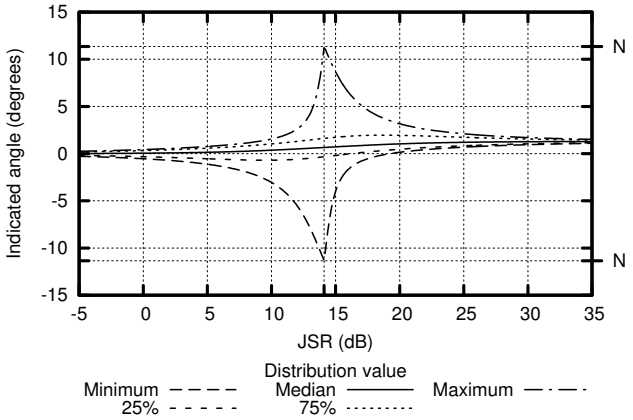

(a) Relative amplitude (a) and phase (ϕ) of 1 dB and 170° respectively.

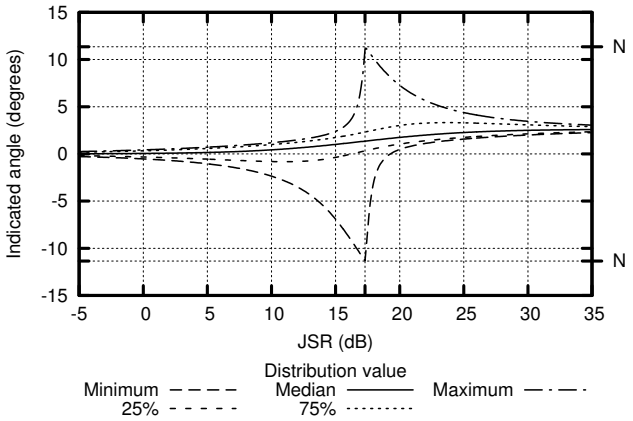

(b) Relative amplitude (a) and phase (ϕ) of 1 dB and 175° respectively.

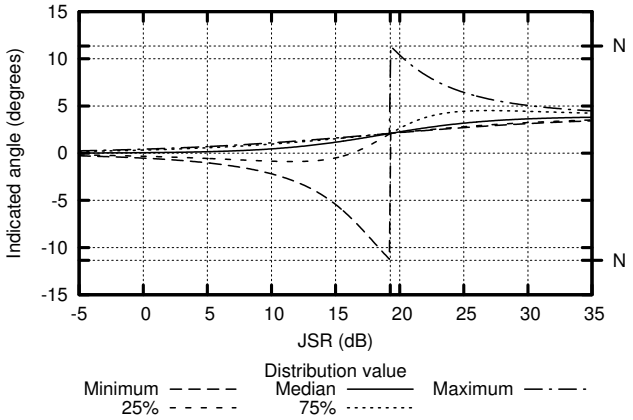

(c) Relative amplitude (a) and phase (ϕ) of 1 dB and 180° respectively.

Fig. 4. Plots showing the indicated angle variation as a function of JSR for the scenario described in the text.

than 1 means that the apparent target created is outside the physical extent of the jammer [29], marking the beginning of the useful range of JSR values. A total cross-eye gain of 2 is exceeded in all cases but one when the JSR is higher than 14 dB. When the JSR is 20 dB, the total cross-eye gain is greater than 4 in all the cases considered except one. These observations support the widely-held view that a JSR of 20 dB is required for a

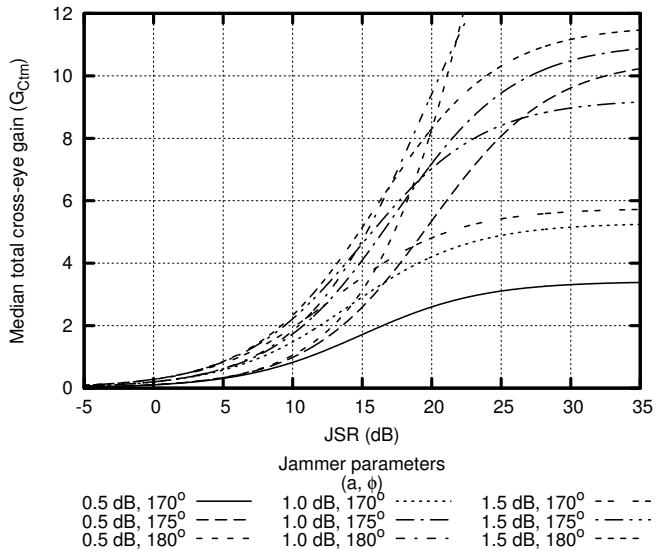

Fig. 5. The median total cross-eye gain as a function of JSR.

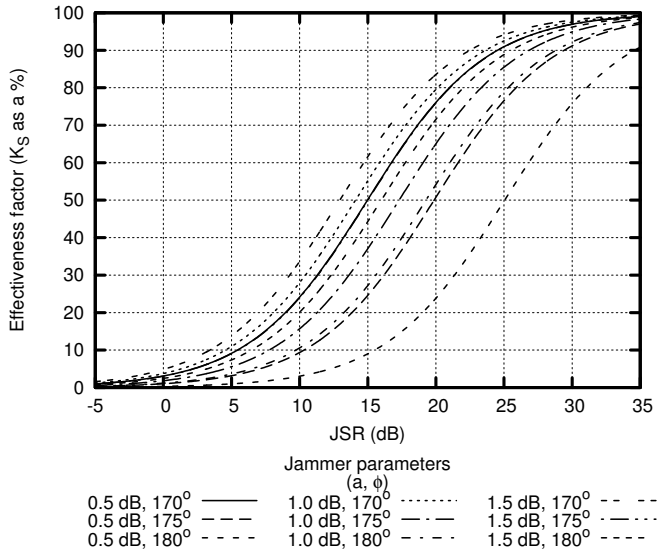

Fig. 6. The effectiveness factor (K_S) as a function of JSR. Note that the 0.5 dB, 170° and 1.5 dB, 175° plots are almost identical.

cross-eye jammer to be effective [3]–[6], and similar conclusions can be reached by considering Fig. 3(a).

The three cases that require the highest JSR values before the total cross-eye gain exceeds 1 are the cases where relative amplitudes of the two directions through the retrodirective cross-eye jammer are 0.5 dB. The total jammer return magnitude in these cases is lower in the other cases because the amplitudes of the two jammer channels are more closely matched. A higher JSR is thus required before the total jammer return magnitude is comparable to the skin return magnitude.

The effectiveness factor (K_S) is plotted against JSR in Fig. 6. These results show that the JSR values of 45 dB and 65 dB to get half and 90% of the isolated cross-eye gain respectively quoted in [10] are extremely conservative because JSRs of only 25 dB and 35 dB respectively are required in all cases in Fig. 6. The

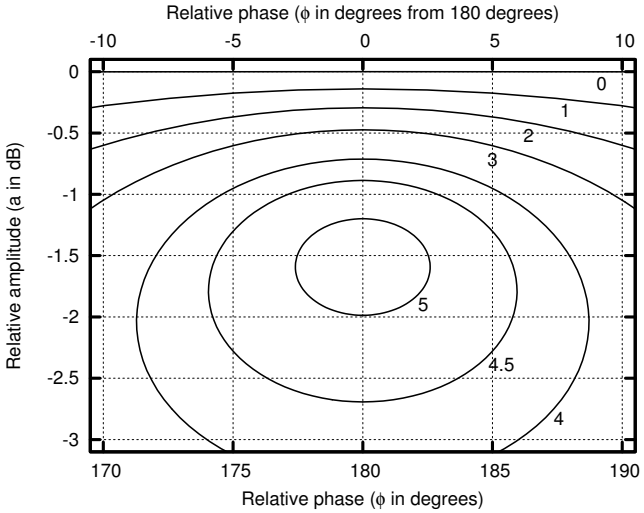

(a) 15 dB JSR.

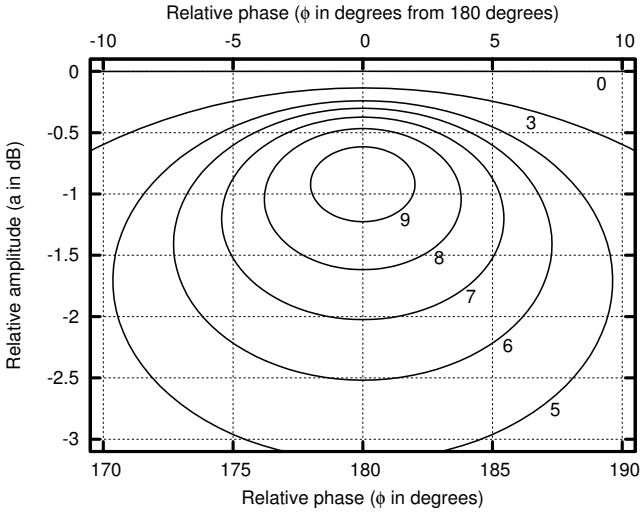

(b) 20 dB JSR.

Fig. 7. Contours of constant median total cross-eye gain (G_{Ctm}) in the presence of platform skin return as a function of the jammer parameters (a and ϕ).

differences are again due to the fact that the analysis in [10] ignores the retrodirective implementation of cross-eye jamming.

Comparing the results in Fig. 6 to those in Fig. 5 shows two conflicting requirements. Fig. 6 shows that larger amplitude and phase mismatches between the two directions through the retrodirective cross-eye jammer cause a higher proportion of the isolated cross-eye gain to be achieved. However, Fig. 5 shows that the total cross-eye gain at high JSR is lower with large amplitude mismatches because the isolated cross-eye gain is also lower. There is thus a compromise between having a large amplitude mismatch to ensure that the jammer's sum-channel return is large and having a small amplitude mismatch to ensure that the total cross-eye gain is high.

Fig. 7 explores this compromise further by plotting contours of constant median total cross-eye gain as a function of the jammer parameters for JSR values of 15 dB and 20 dB. As the amplitude mismatch in Figs 7(a)

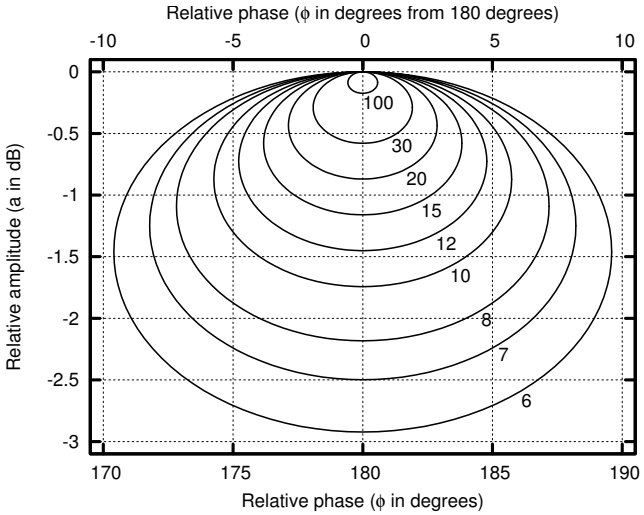

Fig. 8. Cross-eye gain (G_C) contours as a function of the jammer parameters (a and ϕ) in the absence of platform skin return (infinite JSR) from [29].

and 7(b) increases, the total cross-eye gain first increases and then decreases.

The initial increase in median total cross-eye gain magnitude occurs because the magnitude of the total return from the cross-eye jammer increases, so it has a larger effect on the total sum-channel signal. This initial increase is not present when the cross-eye jammer is considered in isolation as in Fig. 8 from [29] because the skin return is not present. The eventual decrease in median total cross-eye gain magnitude occurs because an isolated cross-eye jammer achieves its greatest effect when the amplitude match is close to 0 dB as shown in Fig. 8. The compromise between large amplitude mismatch to achieve a large sum-channel jammer return and small amplitude mismatch to achieve a high isolated cross-eye gain is thus clearly demonstrated.

A further conclusion from comparisons between Figs 7 and 8 is that the total cross-eye gain is significantly lower when platform skin return is present than when the cross-eye jammer is operating in isolation for the JSR values considered. This result is not surprising because the skin return acts as a beacon, counteracting the effect of the cross-eye jammer.

The jammer parameters (a and ϕ) to achieve a specified total cross-eye gain with optimum tolerance to parameter variations are at the centre of the relevant contour in Fig. 7. This occurs at a relative phase of 180° and a relative amplitude determined by solving (34) for a and taking the median to get

$$a = \frac{G_S}{G_S + 1} \tag{44}$$

where G_S is the specified median total cross-eye gain. Surprisingly, this optimum design point is not dependent on the JSR, and more significantly, is identical to the optimal design point for the isolated case [29].

While the JSR does not change the position of the optimum design point, it does determine whether the specified median total cross-eye gain can be achieved and the allowable tolerances. For example, the 15-dB JSR in Fig. 7(a) cannot achieve a median total cross-eye gain of 9, while the 20-dB JSR in Fig. 7(b) can. Furthermore, the contour for a median total cross-eye gain of 5 is much smaller in Fig. 7(a) than in Fig. 7(b) because of the latter's higher JSR.

Finally, Fig. 7(a) shows that median total cross-eye gain values of over 4 can be achieved with relatively large tolerances to component variations when the JSR is 15 dB. Fig. 7(b) shows that increasing the JSR to 20 dB means that very large median total cross-eye gains can be achieved. These results suggest that the value of 20 dB JSR which is widely quoted in the literature [3]–[6] is realistic, though slightly conservative.

IV. Conclusion

An analysis of the performance of a retrodirective cross-eye jammer in the presence of platform skin return is presented. This is believed to be the first published analysis of this case.

The first significant result is that the value of 20 dB JSR for a cross-eye jammer to be effective is reasonable because large median total cross-eye gains are generated in this case. This value agrees with the widely-quoted, though unsubstantiated, JSR value given in much of the cross-eye literature. However, this value can be considered conservative because apparent targets well outside the physical extent of the jammer can be achieved with lower JSR values.

An optimal design point to obtain a specified median total cross-eye gain in the presence of platform skin return with maximum tolerance to jammer parameter variations is proposed. Surprisingly, this point does not depend on the JSR and is identical to the equivalent point for an isolated cross-eye jammer. However, the JSR determines the maximum total cross-eye gain that can be achieved, and the allowable tolerances to achieve the specified gain. Graphs that illustrate the effect of the jammer parameters and JSR are provided.

While extremely useful, the derived result is only valid for a point target that is positioned halfway between the jammer antennas and is thus unable to consider other cases (e.g. jammer antennas not positioned symmetrically around the centre of the platform). Furthermore, only the median case is considered analytically. Additional work is thus required to obtain a complete understanding of the effect of platform skin return on cross-eye jamming.

Appendix

This appendix proves that an equation of the form

$$f = \frac{k_1 + k_2 \cos(\theta) + k_3 \sin(\theta)}{k_4 + k_5 \cos(\theta) + k_6 \sin(\theta)} \tag{45}$$

where k_1 to k_6 are arbitrary constants has a median value given by

$$f_m = \frac{k_1}{k_4} \tag{46}$$

when θ can be any angle with equal probability.

Equation (45) can be rewritten as

$$0 = (k_1 - fk_4) + (k_2 - fk_5)\cos(\theta) + (k_3 - fk_6)\sin(\theta) \tag{47}$$

which can be simplified by defining

$$\cos(\phi) = \frac{k_2 - fk_5}{k_m} \tag{48}$$

$$\sin(\phi) = \frac{k_3 - fk_6}{k_m} \tag{49}$$

$$k_m^2 = (k_2 - fk_5)^2 + (k_3 - fk_6)^2 \tag{50}$$

where both ϕ and k_m are constants, allowing (47) to be rewritten as

$$0 = (k_1 - fk_4) + k_m \left[\cos(\theta)\cos(\phi) + \sin(\theta)\sin(\phi)\right] \tag{51}$$

$$0 = (k_1 - fk_4) + k_m \cos(\theta - \phi) \tag{52}$$

$$0 = (k_1 - fk_4) + k_m \cos(x) \tag{53}$$

where $x = \theta - \phi$. This can be solved for x to give

$$x = n2\pi + \arccos\left[\frac{fk_4 - k_1}{k_m}\right] \tag{54}$$

where n is an arbitrary integer. The value of x that gives a specified value of f denoted f_k is denoted x_k and can be determined from (54).

The cumulative distribution function of x can be written as

$$F_x(x) = \begin{cases} 0 & x \le -\pi \\ \frac{1}{2\pi}(x + \pi) & -\pi < x < \pi \\ 1 & x \ge \pi \end{cases} \tag{55}$$

because this definition ensures that x can have any angle with equal probability, thereby allowing θ to have any angle with equal probability as required.

The cumulative distribution function of f can now be written as

$$F_f(f_k) = P\{f \le f_k\} \tag{56}$$

$$= P\{|x| \le x_k\} \tag{57}$$

$$= F_x(x_k) - F_x(-x_k) \tag{58}$$

$$= \frac{1}{\pi}\arccos\left[\frac{f_k k_4 - k_1}{k_m}\right] \tag{59}$$

where (54) was used to eliminate x_k.

The median of f – f_m – is obtained by setting $F_f = 0.5$ and solving to obtain

$$\frac{1}{2} = \frac{1}{\pi}\arccos\left[\frac{f_m k_4 - k_1}{k_m}\right] \tag{60}$$

$$\cos\left(\frac{\pi}{2}\right) = \frac{f_m k_4 - k_1}{k_m} \tag{61}$$

$$f_m = \frac{k_1}{k_4} \tag{62}$$

which is the desired result.

REFERENCES

[1] P. E. Redmill, "The principles of artificial glint jamming ("cross eye")," Royal Aircraft Establishment (Farnborough), Tech. note RAD. 831, March 1963.

[2] L. B. Van Brunt, *Applied ECM*. EW Engineering, Inc., 1978, vol. 1.

[3] G. E. Johnson, "Jamming passive lobing radars," *Electronic Warfare*, vol. 9, pp. 75–85, April 1977.

[4] D. C. Schleher, *Electronic warfare in the information age*. Artech House, 1999.

[5] D. L. Adamy, *EW 101: A first course in electronic warfare*. Artech House, 2001.

[6] F. Neri, *Introduction to electronic defense systems*. Artech House, 1991.

[7] W. P. du Plessis, J. W. Odendaal, and J. Joubert, "Extended analysis of retrodirective cross-eye jamming," *IEEE Transactions on Antennas and Propagation*, vol. 57, no. 9, pp. 2803–2806, September 2009.

[8] W. P. du Plessis, "A comprehensive investigation of retrodirective cross-eye jamming," Ph.D. dissertation, University of Pretoria, 2010.

[9] W. P. du Plessis, J. W. Odendaal, and J. Joubert, "Experimental simulation of retrodirective cross-eye jamming," *IEEE Transactions on Aerospace and Electronic Systems*, vol. 47, no. 1, pp. 734–740, January 2011.

[10] R. N. Lothes, M. B. Szymanski, and R. G. Wiley, *Radar vulnerability to jamming*. Artech House, 1990.

[11] A. Golden, *Radar Electronic Warfare*. AIAA Inc., 1987.

[12] L. Falk, "Cross-eye jamming of monopulse radar," in *IEEE Waveform Diversity & Design Conf.*, 4-8 June 2007, pp. 209–213.

[13] S. A. Vakin and L. N. Shustov, "Principles of jamming and electronic reconnaissance - volume I," U.S. Air Force, Tech. Rep. FTD-MT-24-115-69, AD692642, 1969.

[14] A. I. Leonov and K. I. Fomichev, "Monopulse radar," U.S. Air Force, Tech. Rep. FTD-MT-24-982-71, AD742696, 1972.

[15] J. W. Wright, "Radar glint – a survey," *Electromagnetics*, vol. 4, no. 2, pp. 205–227, January 1984.

[16] D. D. Howard, "Tracking radar," in *Radar Handbook*, 2nd ed., M. I. Skolnik, Ed. McGraw-Hill, 1990, ch. 18.

[17] ——, "Radar target angular scintillation in tracking and guidance systems based on echo signal phase front distortion," in *Proc. Nat. Eng. Conf.*, vol. 15, 1959, reprinted in Radars, Vol. 4, Radar Resolution & Multipath Effects, David K. Barton, Ed., Artech House, 1975.

[18] J. E. Lindsay, "Angular glint and the moving, rotating, complex radar target," *IEEE Transactions on Aerospace and Electronic Systems*, vol. 4, no. 2, pp. 164–173, March 1968.

[19] J. H. Dunn and D. D. Howard, "Radar target amplitude, angle, and doppler scintillation from analysis of the echo signal propagating in space," *IEEE Transactions on Microwave Theory and Techniques*, vol. 9, no. 9, pp. 715–728, September 1968.

[20] S. M. Sherman, "Complex indicated angles applied to unresolved radar targets and multipath," *IEEE Transactions on Aerospace and Electronic Systems*, vol. 7, no. 1, pp. 160–170, January 1971.

[21] ——, *Monopulse principles and techniques*. Artech House, 1984.

[22] H. Yin and P. Huang, "Unification and comparison between two concepts of radar target angular glint," *IEEE Transactions on Aerospace and Electronic Systems*, vol. 31, no. 2, pp. 778–783, April 1995.

[23] P. J. Kajenski, "Comparison of two theories of angle glint: polarization considerations," *IEEE Transactions on Aerospace and Electronic Systems*, vol. 42, no. 1, pp. 206–210, January 2006.

[24] H. C. Yin and P. K. Huang, "Further comparison between two concepts of radar target angular glint," *IEEE Transactions on Aerospace and Electronic Systems*, vol. 44, no. 1, pp. 372–380, January 2008.

[25] F. Neri, "Considering cross-eye," Letter to the Journal of Electronic Defence, June 2007.

[26] Y. Stratakos, G. Geroulis, and N. Uzunoglu, "Analysis of glint phenomenon in a monopulse radar in the presence of skin echo and non-ideal interferometer echo signals," *Journal of Electromagnetic Waves and Applications*, vol. 19, no. 5, pp. 697–711, 2005.

[27] W. P. du Plessis, J. W. Odendaal, and J. Joubert, "Generality of an extended cross-eye jamming analysis," *IEEE Transactions on Aerospace and Electronic Systems*, rejected.

[28] M. R. Spiegel and J. Liu, *Mathematical Handbook of Formulas and Tables*, 2nd ed., ser. Schaum's Outline Series. McGraw-Hill, 1999.

[29] W. P. du Plessis, J. W. Odendaal, and J. Joubert, "Tolerance analysis of cross-eye jamming systems," *IEEE Transactions on Aerospace and Electronic Systems*, vol. 47, no. 1, pp. 740–745, January 2011.

Warren du Plessis (M'00, SM'10) received the B.Eng. (Electronic) and M.Eng. (Electronic) and Ph.D. (Engineering) degrees from the University of Pretoria in 1998, 2003 and 2010 respectively, winning numerous academic awards including the prestigious Vice-Chancellor and Principal's Medal.

He spent two years as a lecturer at the University of Pretoria, and then joined Grintek Antennas (since split between Poynting Antennas and Saab EDS) as a design engineer for almost four years. Since 2006, he has been working in electronic warfare (EW) at Defence, Peace, Safety and Security (DPSS), a division of the Council for Scientific and Industrial Research (CSIR) in Pretoria, South Africa. His primary research interests are cross-eye jamming, and thinned and sparse antenna arrays.